Implementation of Adaptive Wavelet Thresholding and Non-local Means for Medical Image Enhancement for Noise Reduction

Prerna Mamgain[1], Sachin Chaudhary[2]

Department of Information Technology, DIT University
Dehradun, Uttarakhand, India

Abstract: *Images are most widely used for radiological diagnosis in medical examinations. The presence of artifacts and noise in images causes the difficulty in medical diagnosis. The noises are generally occurred and corrupt an image during its acquisition or transmission. Image denoising is one of the popular methods with an aim of noise reduction to retain images quality. In this paper, Wavelet based noise reduction technique is proposed to improve image quality where thresholding and Non-local means algorithm are applied. The Noisy medical image is decomposed using DWT, where approximation part is filtered using Non-local means filter and detail parts are filtered by the thresholding. By using the level dependent, the wavelet coefficients are calculated using optimal linear interpolation shrinkage function. Denoised image is acquired using inverse DWT. The value of the peak signal to noise ratio (PSNR) is used as the measure of image visual quality.*

Keywords**:** *DWT, PSNR, denoising, thresholding, decomposition.*

I. INTRODUCTION

1.1 General

Digital image processing plays a key role in medical diagnosis. Medical images are obtained and analyzed to determine the presence or absence of abnormalities such as tumor, which is vital in understanding the type and magnitude of a disease. Unfortunately, medical images are susceptible to impulse noise during acquisition, storage and transmission. Hence, image denoising is a primary precursor for medical image analysis tasks. Conventional smoothening filters and median filters are the most popular filters for noise reduction in digital images. But, a single smoothening or median filter is not enough for completely removing the noise, especially when the noise level is high. Also, it may not preserve image details such as edges during filtering. This is a serious issue in medical image analysis because loss of image details results in inaccurate image analysis which may prove fatal to the life of a person. Applying a set of denoising and enhancement filters successively on a noisy image may remove noise and preserve image details much more efficiently than a single median or smoothening filter. We proposed an approach which is used to enhance a medical image by using Haar and db3 wavelet transform, by selecting soft and hard thresholding level and thus reducing the noise. In this paper, unwanted noisy components can be thresholded without affecting the significant features of the image. We calculate PSNR (Peak Signal To Noise Ratio) and MSE (Mean Square Error) by using these two orthogonal wavelets and then compare the resultants.

II. CLASSIFICATION OF DENOISING

Digital images plays vital role in day to day applications. Noise is introduced in the images during transmission and acquiring from cameras. Any unwanted signal and its electrical interference and blur due to camera movement, environmental conditions like rain, snow, and sampling and quantization errors could be considered as noise. In other terms one person's signal might be another person's noise. The noise complicates the post process of compression and other image processing tasks. So it becomes very essential to remove noise for better interpretation by human eyes. There are two types of noise namely multiplicative noise and additive noise. The multiplicative noise is generally complex model and caused by de-phased echo signals from scatters. It is image dependent and difficult to reduce noise though it contains useful information.

There are other kinds of noise called additive noise which is systematic and easy to model and noise can be removed with less effort.
An additive noise model is represented as
$z(x, y) = s(x, y) + n(x, y)$

The multiplicative noise satisfies

$$z(x, y) = s(x, y) \times n(x, y)$$

where s(x,y) is the original signal information, n(x,y) represents the noise introduced into the signal and the output produced the corrupted image z(x,y), and (x,y) represents the pixel location. Image addition finds applications in image morphing. The multiplication alters the brightness of the image.

2.1 Image Noise Types:

a) Gaussian Noise

The standard model of amplifier noise is Gaussian, addictive, free at each pixel, and free of signal intensity caused mostly by thermal noise, including which comes from rearranging capacitors. In color cameras where additional amplification is used there can be more noise in the channel. Amplifier noise is a most important component of the "read noise" of an image sensor.

b) Salt-and-Pepper Noise:

Fat-tailed distributed or “impulsive” noise is sometimes called as salt-and-pepper noise. An image containing salt-and-pepper noise will have dark pixels in bright regions and bright pixels in dark regions. This type of noise can be caused by ADC errors, bit errors in transmission, etc. lifeless pixels in an LCD screen produce a like, but non-random, display. This can be eliminated in huge part by using dark/bright pixels.

c) Poisson Noise:

The dominant noise in the lighter parts of the image from a image sensor is characteristically that caused by statistical quantum changes, i.e., variety in the measure of photons sensed at a given disclosure level; this noise is called as photon shot noise. Short noise has a root-mean-square value relative to the square root of the image intensity, and the noises at dissimilar pixels are independent of one more. Shot noise follows a Poisson distribution, which is usually not very unlike from Gaussian. Notwithstanding photon shot clamor, there can be current in the image sensor; this noise is sometimes known as "dark-current shot noise" or "dark shot noise".

d) Speckle Noise:

Speckle noise is multiplicative shot additional noise from the dark spillage commotion. This sort of clamor happens in pretty much all coherent imaging system.

The source of this noise is attributed to random interference between the coherent returns. Speckle noise has the characteristic of multiplicative noise and obeys distribution given as:

$$f(g) = \left\{ \frac{g^{a-1}}{(\alpha-1)!\,\alpha^{\alpha}} \right\} e^{-\frac{g}{a}}$$

Where variance is a 2α and g is the gray level.

2.2 Image Denoising

Filtering is perhaps the most fundamental process of image processing and computer vision. In the broad sense of term “filtering”, ", the value of the filtered image at a given location is a function of the values of the input image in a small neighborhood of the same location. For example, Gaussian low-pass filtering computes a weighted average of pixel values in the neighborhood, in which the weights decrease with distance from the neighborhood center. Although formal and quantitative explanations of this weight fall-off can be given, the intuition is that images typically vary slowly over space, so near pixels are likely to have similar values, and it is therefore appropriate to average them together. The noise values that corrupt these nearby pixels are mutually less correlated than the signal values, so noise is averaged away while signal is preserved. However, the assumption of slow spatial variations fails at edges, which are consequently blurred by linear low pass filtering.

The denoising is an operation to estimate clean image from a degraded or noise affected image and this process is required to achieve visually pleasant and also to get quality reconstruction of image.

The aim of the paper is to improve the medical image quality which is degraded through noise.

To improve the image quality, noise reduction techniques are used over lower dose images and noise is reduced with preserving all clinically relevant structures.

The major challenges for noise reduction in CT Image are:

- Flat regions should be flat
- Image boundaries should be preserved (no blurring)
- Texture details should be preserved
- Global contrast should be maintained

Artifacts should not be appeared**.**

III. PROPOSED TECHNIQUE

With this assumption the medical image is corrupted by Gaussian noise with zero mean and variance as following equation, the noisy image can be expressed as:

$B(i,j)_s = A(i,j)_s + \eta(i,j)_s$……………………………(3.1)

Where, $\eta(i,j)_s$ is noise coefficient, $A(i,j)_s$ is noiseless image and $B(i,j)_s$ is noisy image.

Noise reduction architecture is proposed as shown in figure 4.1, where following steps are processed as:

Step 1: Perform discrete wavelet transform (DWT) of medical image corrupted by Gaussian noise to obtain approximation and detail parts.

Step 2: Estimate decomposition level by using log energy.

Step 3: Apply adaptive wavelet based thresholding over the detail parts.

(i) Compute the threshold value for each sub-band in all levels.

(ii) Apply Threshold to all sub-band’s coefficients using the optimum linear interpolation threshold function.

Step 4: Apply Non-local Means method over approximation part.

Step 5: Perform inverse discrete wavelet transform (IDWT) using step 3 & 4.

In the above algorithm, the two way denoising method is used. One part (approximation) is denoised by Non-local means and other part (detail) is denoised by thresholding using optimum linear interpolation method. Using both results, reconstruction is done to get the final denoised image.

3.1 Extraction of Decomposition level

After defining cost function, the wavelet packet decomposition is done with following steps:

1) Firstly, set the maximum number of levels.

2) For each level, decompose into four sub-bands (child nodes).

3) Compute cost value for each sub-band for each level.

4) In top down approach manner, Check the cost value:

   a) If the cost of parent node is greater than total cost of child nodes; do continue.

   b) Otherwise; eliminate children nodes.

5) End the process, if there is no node to decompose.

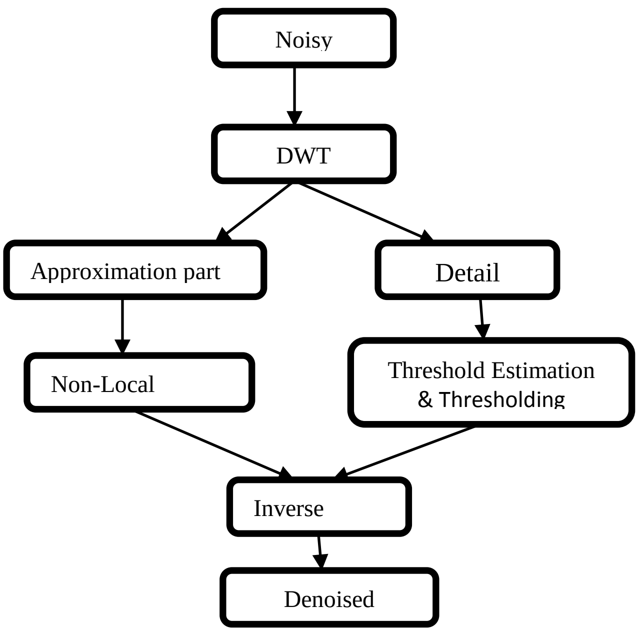

Figure 3.1: Proposed noise reduction architecture

3.2 Image denoising by Non-local Means

Each pixel p of the non-local means denoised image is computed with the following formula:

$$NL(V)(p) = \sum_{q \epsilon V} w(p,q)V(q) \ldots\ldots\ldots\ldots\ldots\ldots (3.2)$$

Where V is the noisy image, and weights w(p,q) meet the following conditions $0 \leq w(p,q) \leq 1$ and $\sum_q w(p,q) = 1$. Each pixel is a weighted average of all the pixels in the image. The weights are based on the similarity between the neighborhoods of pixels p and q. For example, in Figure 4.1 above the weight $w(p,q_1)$ is much greater than $w(p,q_2)$ because pixels p and q_1 have similar neighborhoods and pixels p and q_2 do not have similar neighborhoods. In order to compute the similarity, a neighborhood must be defined. Let N_i be the square neighborhood centered about pixel i with a user-defined radius R_{sim}. To compute the similarity between two neighborhoods take the weighted sum of squares difference between the two neighborhoods or as a formula:

$$d(p,q) = ||V(N_p) - V(N_q)||_2^2, \ F[1, 2] \ldots\ldots\ldots\ldots\ldots\ldots (3.3)$$

F is the neighborhood filter applied to the squared difference of the neighborhoods and will be further discussed later in this section. The weights can then be computed using the following formula:

$$w(p,q) = (\frac{1}{Z(p)})e^{\frac{-d(p,q)}{h}}] \ldots\ldots\ldots\ldots\ldots\ldots\ldots\ldots\ldots\ldots (3.4)$$

Z(p) is the normalizing constant defined as:

$$Z(p) = \sum_q e^{\frac{-d(p,q)}{h}}] \ldots\ldots\ldots\ldots\ldots\ldots\ldots\ldots\ldots\ldots\ldots\ldots (3.5)$$

Where h is the weight-decay control parameter.

As previously mentioned, F is the neighborhood filter with radius Rsim. The weights of F are computed by the following formula:

$$\frac{1}{R_{sim}} \sum_{i=m}^{R_{sim}} 1/(2*i+1)^2] \ldots\ldots\ldots\ldots\ldots\ldots\ldots\ldots (3.6)$$

Where m is the distance the weight is from the center of the filter. The filter gives more weight to pixels near the center of the neighborhood, and less weight to pixels near the edge of the neighborhood. The center weight of F has the same weight as the pixels with a distance of one. Despite the filter's unique shape, the weights of filter F do sum up to one.

3.3 Thresholding Based Denoising

The steps of threshold based denoising are:

(1) In Wavelet decomposition, a wavelet is chosen for determining its decomposing layers such as haar, db2, etc.

(2) Decomposition level is extracted according to optimal base of wavelet packet by calculating cost value of parent node and child nodes with help of log energy function.

(3) Select an optimum threshold value and do the thresholding to the coefficient of each sub-band for each level.

(4) After thresholding on all sub-bands for all levels, do wavelet reconstruction.

3.4 Threshold Selection

For CT images, selection of a threshold value is not an easy task. By selecting small threshold value, the result image may be noisy. And for large threshold value, the result image may be blurring. Both are not good for denoising. An optimal threshold algorithm is used for the selection of threshold and used as:

$$\lambda(s) = SW\left(\frac{\sigma}{\sigma_{A,s}}\right)] \ldots\ldots\ldots\ldots\ldots\ldots\ldots\ldots (3.7)$$

Where the noise variance can be estimated, as:

$$\sigma_s^2 = \left[\frac{median\ (|B(i,j)_S|)}{0.6745}\right]^2 \ldots\ldots\ldots\ldots\ldots\ldots\ldots (3.8)$$

Where, $\sigma_{A,s}$is variance of noiseless image for each sub-band and SW represents the weight value for each sub-band to all levels. SW can be calculated by addition of weight value for sub-band of horizontal and vertical direction.

3.5 Thresholding Algorithm

After selecting a threshold value, the process of thresholding is applied by selecting an appropriate algorithm. Hard thresholding and soft thresholding methods are very popular for thresholding. In hard threshold, each coefficient value is compared with threshold value and less than value is replaced by zero. In Soft threshold, replaced by zero process is same as in hard threshold, additionally rest of coefficients are modified by subtracting threshold values. In comparison of both, Soft thresholding gives better performance for visual appearance of images. But soft thresholding has a limitation with large coefficient values.

To overcome those limitations, an optimal linear interpolation (OLI) shrink algorithm is used for thresholding.

$$OL_{\lambda_s}^{(B(i,j)_S)} = \begin{cases} 0, & |B(i,j)_s| \le \lambda_s \\ B(i,j)_s - \left(\frac{\sigma^2}{\sigma_{B,s}^2}\right)(B(i,j)_s, -\mu_s), & |B(i,j)_s| > \lambda_s \end{cases}$$

……………(3.9) Where, $\mu_s$is the mean value of the sub-band. The above thresholding function is obtained by combining the Shrink technique with the Bayesian MAP estimation.

IV. RESULT AND ANALYSIS

The experimental evaluation is performed on medical images is using two categories: synthetic (computer generated) and real medical image with size 512x512. Synthetic image as shown in Figure 4.1(a) is a phantom image, most widely used in image reconstruction.

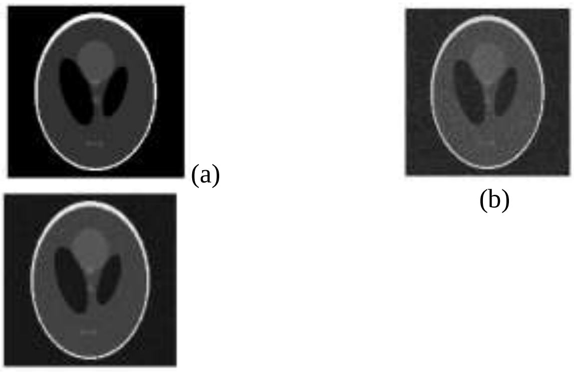

Figure 4.1: (a) Synthetic image
(b) Additive Gaussian noise synthetic image
(c) Denoised synthetic image

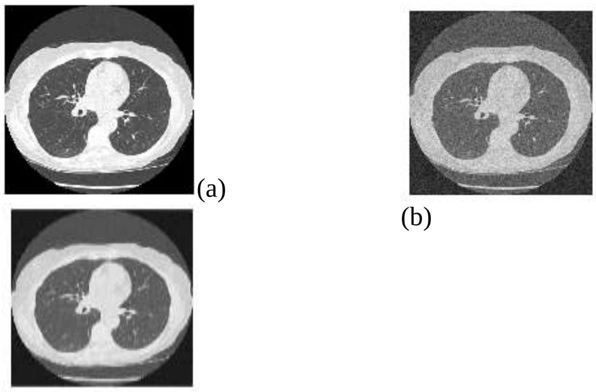

Figure 4.2: (a) Real image (First)
(b) Additive Gaussian noise image (First)
(c) denoised image (First)

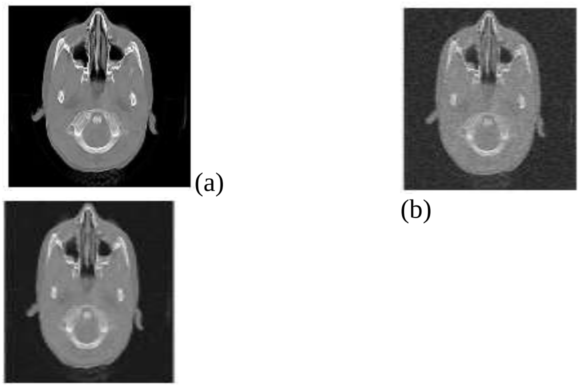

Figure 4.3: (a) Real image (Second)
(b) Additive Gaussian noise image (Second)
(c) Denoised image (Second)

(a)

(b)

(c)

Figure 4.4: (a) Real image (Third)
(b) Additive0 Gaussian noise image (Third)
(c) Denoised image (Third)

The zero mean Gaussian noise with varying standard deviation is added on synthetic as well as real medical images to generate noisy images. The generated noisy images with a Gaussian noise of mean zero & standard deviation 30 are shown in Figure 4.1(b), 4.2(b), 4.3(b) & 4.4(b). The Haar wavelet transform is applied to decompose the image into approximation and detail parts. Now, Two-way denoising method is applied. Final denoised medical image can be obtained by inverse wavelet decomposition. The reconstructed results are shown in Figure 4.1(c), 4.2(c), 4.3(c) & 4.4(c). The quality performances of medical images are measured by:

$$PSNR = 10\log_{10}\frac{255^2 mn}{\sum_{j=1}^{m}\sum_{i=1}^{n}[B(i,j)-B(i,j)]^2}$$

dB……………………(4.1)

Where m & n are the number of pixels in each column and row, respectively, B(i, j) and B(i, j) are the original and reconstructed images.

V. CONCLUSION

The proposed method is applied on the basis of two-way filtering using wavelet thresholding and NLM filtering. PSNR of proposed methods is indicating that PSNR decreases with the increasing values of standard deviation of Gaussian noise. Although the computed PSNR values are satisfactory good and the mean error values are very small. Experimental results demonstrate significantly better image visual quality by reducing noise and reserving edges. The PSNR value and mean error indicating better performance of proposed method for additive Gaussian noise in synthetic as well as real medical images. The resultant images are in good quality for clinical diagnosis and may be supported for clinical applications by providing further control over image quality and analysis.

VI. REFRENCES

[1] M. K. Kalra, M. M. Maher and T. L. Toth, “Strategies for CT radiation dose optimization,” Journal of Radiology, vol. 230, no.3, pp. 619-628, 2004.

[2] S. G. Chang, B. Yu and M. Vetterli, “Adaptive wavelet thresholding for image denoising and compression,” IEEE Trans. on Image Proc., vol. 9, no. 9, pp. 1532-1546, 2000.

[3] S. Mallat, “A theory for multiresolution signal decomposition: the wavelet representation,” IEEE Trans. on Pattern Anal. Mach. Intell., vol. 11, pp. 674-693, no. 7, 1989.

[4] M. Nasri and H. Nezamabadi-Pour, “Image denoising in the wavelet domain using a new adaptive thresholding function,” Neurocomputing, vol. 72, nos. 4–6, pp. 1012–1025, 2009.

[5] D. L. Donoho and I. M. Johnstone, “Ideal spatial adaptation via wavelet shrinkage,” Biometrika, vol. 81, no. 3, pp. 425–455, 1994.

[6] Sankur B. and Sezginb M. “Image Thresholding Techniques: a Survey over Categories,” Journal of Electronic Imaging, vol. 13, no. 1, pp. 146-165 2004.

[7] K. Li and R. Zhang, “Multiscale wiener filtering method for low-dose CT images,” IEEE Biomedical Engineering and Informatics, New York pp. 428–431, 2010.

[8] Cheng-Ting Shih, Shu-Jun Chang, Yan-lin Liu and Jay Wu " Noise reduction of low-dose computed tomography using the multi-resolution total variation minimization algorithm, " Proc. SPIE, Physics of Medical Imaging, Vol. 8668, 2013.

[9] A. Borsdorf, S. Kappler and R. Raupach, “Analytic noise propagation for anisotriopic denoising of CT images,” IEEE Nucl Sci Symp Conf Rec, pp. 5335–5338, 2008.

[10] J. Saeedi and M. H. Moradi, “A new wavelet-based fuzzy single and multi-channel image denoising,” Image Vis. Comput., vol. 28, no. 12, pp. 1611–1623, 2010.

[11] L. Shui, Z. F. Zhou, and J. X. Li, “Image denoising algorithm via best wavelet packet base using Wiener cost function,” IET Image Process., vol. 1, no. 3, pp. 311–318, 2007.

[12] Yunhong Li, Xin Yi, Jian Xu and Yuxuan Li, “Wavelet packet denoising algorithm based on correctional wiener filtering,” Journal of Information and Computational Science, vol. 10, no. 9, pp. 2711-2718, 2013.

[13] A. Fathi and A. R. Naghsh-Nilchi, “Efficient image denoising method based on a new adaptive wavelet packet thresholding function,” IEEE Trans Image Process, vol. 21, no. 9, pp. 3981-90, 2012.

[14] A. Buades, B. Coll, J.M. Morel, A review of image denoising algorithms, with a new one, Multiscale Model. Simul. 4 (2005) 490–530.

[15] J.V. Manjon, M. Robles, N.A. Thacker, Multispectral MRI de-noising using nonlocal means, Med. Image Understand. Anal. (MIUA) (2007) 41–46.

[16] J.V. Manjón, J. Carbonell-Caballero, J.J. Lull, G. García-Martí, L. Martí-Bonmatí, M. Robles, MRI denoising using non-local means, Med. Image Anal. 12 (2008) 514–523.

[17] P. Coupe, P. Yger, C. Barillot, Fast non local means denoising for MR images, in: Proceedings at the 9th International Conference on Medical Image Computing and Computer assisted Intervention (MICCAI), Copenhagen, 2006, pp. 33–40.

[18] P. Coupe, P. Yger, S. Prima, P. Hellier, C. Kervrann, C. Barillot, An optimized blockwise nonlocal means denoising filter for 3-D magnetic resonance images, IEEE Trans. Med. Imaging 27 (2008) 425–441.

[19] P. Coupe, P. Hellier, S. Prima, C. Kervrann, C. Barillot, 3D wavelet subbands mixing for image denoising, Int. J. Biomed. Imaging (2008), http://dx.doi.org/10.1155/2008/590183, Article ID 590183.

[20] N. Wiest-Daesslé, S. Prima, P. Coupé, S.P. Morrissey, C. Barillot, Nonlocal means variants for denoising of diffusion-weighted and diffusion tensor MRI, Med. Image Comput. Comput. Assist. Interv. (2007) 344–351.

[21] Rupinderpal Kaur, Rajneet Kaur"Image Denoising Based on Wavelet Technique using Thresholding forMedical Images"International Journal of Computer Trends and Technology (IJCTT),V4(8) August Issue 2013.